Bull. Astr. Soc. India (2002) **30**, 361–366

Optimum Image Parameter ranges for TACTIC Imaging Element: guidance from simulations

M.K.Koul, S.K.Charagi, R.C.Rannot, M.L.Sapru and C.L.Bhat

Bhabha Atomic Research Centre, Nuclear Research Laboratory, Mumbai-400085, INDIA

Abstract. In this paper, we present some results on the performance characteristics of the TACTIC Imaging Element (IE) as predicted by extensive simulation studies. The main features studied are the optimum image parameter ranges for selection of gamma-ray showers from point-sources, corresponding Quality factor (Q) and the gamma-ray image threshold energy of the experiment.

Keywords : Atmospheric cascade simulation; Gamma rays; Atmospheric Cerenkov Technique; Imaging Cerenkov Telescope; Energy Threshold

1 Introduction

In TeV γ-ray astronomy experiments, which are based on detection of atmospheric Cerenkov light, the dominant background comprises cosmic-ray events which outnumber signal events (γ -rays) from a typical point-source by at least a factor of $\sim$ 100. Both, γ-ray and background particles produce cascades in the atmosphere wherein the majority of secondary particles are absorbed in the atmosphere before they can reach the observational ground-level. Nevertheless, these cascades can be efficiently detected via Cerenkov light generated by the passage of charged secondary particles through the air. Using large light collectors in conjunction with fast photomultiplier tube (PMT) arrays and appropriate back-end electronics, these cascades can be detected in the form of Cerenkov images during moonless, clear nights. The Cerenkov image processing and classification schemes, so far used, are mainly based on calculation of second moments of the image, like the Hillas image parameters [1], or its improved Supercuts or extended supercuts versions. In this paper, we have evaluated the figure of merit or quality factor (Q) for the IE of the TACTIC.

2 TACTIC Imaging Element

TACTIC, which stands for TeV Atmospheric Cerenkov Telescope with Imaging Camera [2], is India's first array of imaging γ-ray telescopes. Experimental details of this 4-element array, recently set-up at Mt. Abu, Western India (24.65^o N, 72.7^o E, 1300 m asl), have been discussed elsewhere [3]. The imaging camera of the IE consist of 349 fast photomultiplier tubes (PMT), placed in a closely-packed 19 $\times$ 19 square matrix geometrical configuration (with truncated corners) to cover a FoV of $\sim 6^o \times 6^o$ with a uniform pixel granulation of $\sim 0.31^o$. The PMT are provided with metallic light-guides on the front side to ensure a uniform light collection efficiency by the PMT pixels over a large range of angles of incidence ($< 20^o$) from the light collector. The event triggers are generated from within the central 240 pixels of the imaging camera, leading to a

trigger FoV of $\sim 5^o$ as against an overall image FoV $\sim 6^o$. These triggers are topological proximity triggers of Nearest Neighbour Non-Collinear Triplet (3NCT) type [4].

3 CORSIKA-generated data-bases

The data-bases for carrying out the present studies were generated using the CORSIKA (Version 5.62) air-shower code with Cerenkov option [5]. A total of 5373 showers (429840 events), of either progenitor type, have been considered, as per the differential energy spectrum with an exponent of $\sim$ -2.7, between the energy ranges 0.5TeV - 6.0TeV (γ-rays), and 1.0TeV - 12.0TeV (protons). The methodology followed for TACTIC simulations using the CORSIKA code has been described in the accompanying paper [6]. The photons reflected from a given light collector are ray-traced into the imaging camera pixels. For each progenitor energy value E_p, the total number of events are first sampled as per $\sim$ RdR scaling, where R is the distance of the IE from the centre of the array, and the number of events thus obtained are 220542 for each progenator. Then a trigger event is recorded when each of the 3NCT pixels record $\geq$ 6pe simultaneously. This gives the basic data-base comprising 30346 and 16382 images for γ-rays and protons respectively The data-bases of resulting photoelectron (pe) distributions are subjected to the Cerenkov image analysis. The parameters calculated are the image size (S), Length (L), Width (W), Distance (D) and Alpha (α), as per the supercuts prescription given by Fegan [7].

4 Results

4.1 Lateral Distribution of Cerenkov radiation

Our results on lateral distribution profiles of Cerenkov light,i.e., photon density as a function of the shower core distance, are shown in Fig.1 for γ-ray and proton primaries for several representative progenitor energy values. The average picture shown here is marked by the following prominent features: the mean photon density for γ-rays is nearly uniform for core-distance R upto $\sim$125 m, where it displays a prominent, energy -dependent hump feature. Beyond R $\sim$ 150 m, the photon density decreases, particularly steeply for R $>$ 200 m. On the other hand, the average photon density profile for cosmic-ray protons does not show any hump feature, but falls more or less continuously with the core distance. These results are found to be consistent with the results published by other groups on the topic [8]

4.2 Cerenkov Image Distributions

The 2-dimensional distribution of photoelectrons (pe), thus resulting in the telescope focal plane of the IE, represents the Cerenkov light image due to a gamma-ray or proton primary. The total number of pe present in an image is called the image size (S) and it is a function of the primary type, energy, core distance and its arrival direction or, more precisely, its zenith angle. For the event samples used in the present studies (for which these parameters are pre-fixed), we have plotted in Fig.2 image mean-size ($< S >$) as

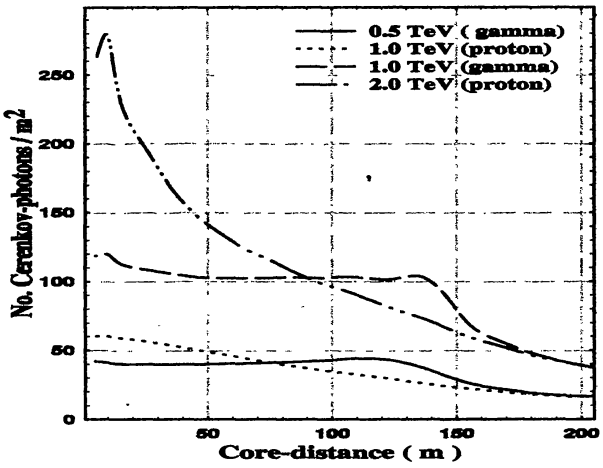

Figure 1: Average lateral distribution profiles of Cerenkov light, i.e., Cerenkov photon density as a function of shower core-distance. Plots are shown for several representative values of progenitor energies. The zenith-angle for the progenitor arrival direction is taken as 20^o.

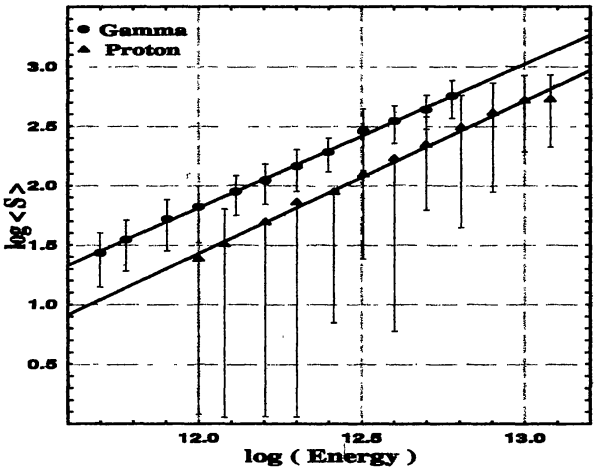

Figure 2: Plots of Cerenkov image average size $< S >$, and the corresponding $\pm 1\sigma$ standard deviation limits, plotted as a function of the primary energy (in eV) for γ-rays and protons. The core-distance range considered is R $\sim$ 35m - 135m.

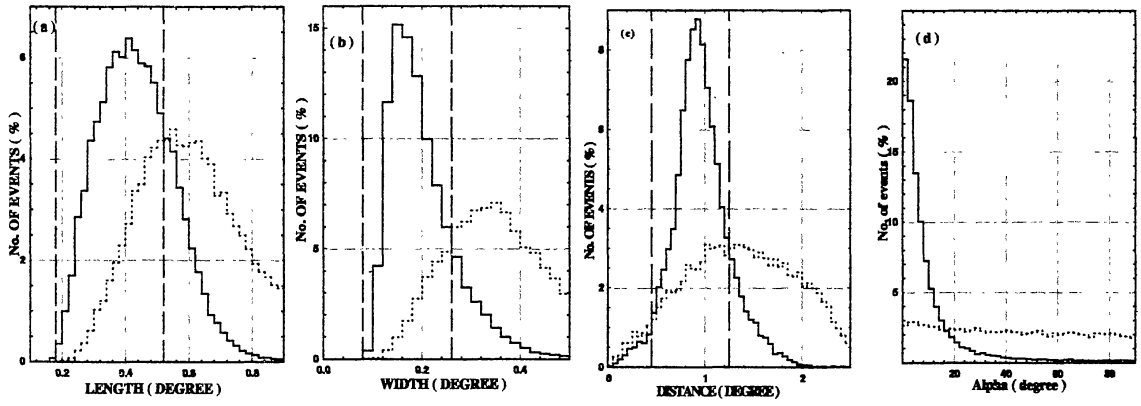

Figure 3: Distributions of typical image parameters as predicted for the 19 × 19 pixel imaging camera of the TACTIC for γ-rays (0.5 - 6.0 TeV) and proton primaries (1.0 - 12.0 TeV) : Length (L): a; Width (W): b; Distance (D): c; and Alpha (α): d.

a function of the primary energy for γ-rays and protons separately. The core-distance parameter (R) has been chosen to lie between 35 m $\leq$ R $\leq$ 135 m, the range over which the lateral photon density profile is seen to be rather flat for γ-rays. The following two well-behaved power- law fits are obtained between the mean-size ($< S >$) and primary energy E (eV) for gamma-ray and proton progenitors respectively:

$$log < S >= (1.208 \pm 0.075) log(E) - (12.687 \pm 0.137) \quad (1)$$

$$log(< S >) = (1.284 \pm 0.127) log(E) - (13.981 \pm 0.631) \quad (2)$$

It is evident that $< S >$ is not exactly linearly related to the primary particle energy but follows more closely a power-law with a non-unity exponent. This somewhat unexpected result also follows from the work of [9]. Further, the typical errors expected for γ-ray events are smaller ($\sim$ 30 %) than for proton events (> 60%), mainly because of the different forms of the average lateral distribution functions.

Cerenkov images have embedded in them signatures which are related to details of interactions of the progenitor particle and its secondaries in the atmosphere. Using the standard moments-fitting procedure [10], these images can be parameterized and the typical parameters calculated using the recently-developed, supercuts image classification strategy, which is based on image-shape parameters like image Length (L), Width (W) and Distance (D) as well as the image orientation-parameter, Alpha (α). Figure 3 presents results on the L, W, D and α distributions, for both gamma-ray and proton images, combined for different primary energies considered here. It is clear from the figure that the shape parameter distribution corresponding to the proton events are broader and bigger as compared with the corresponding values for gamma-rays.

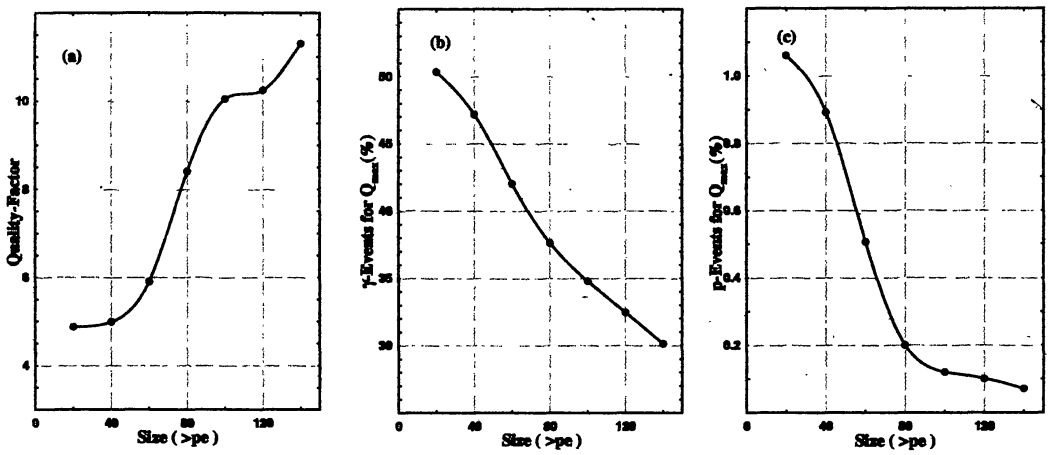

Figure 4: Variation of the Imaging Element quality-factor Q ($\alpha \leq 15^o$) with the image size (a). The corresponding percentages of γ-ray and proton images retained are shown in (b) and (c) respectively.

4.3 Sensitivity estimates of TACTIC Imaging Element

In keeping with the standard practice in the field, the expected sensitivity of the TACTIC Imaging Element (IE), can be quantified by its quality factor or figure of merit Q, defined as:

$$Q = \frac{\frac{N_\gamma}{N_{\gamma t}}}{\sqrt{\frac{N_p}{N_{pt}}}} \qquad (3)$$

where $N_{\gamma t}$ and N_{pt} are the total numbers of gamma-ray and proton images respectively, considered in the analysis here, and N_γ and N_p are the corresponding numbers which survive the optimized cut values, obtained for the above-referred image-parameters, viz, L, W, D and α. To compute Q, we have chosen boundaries for L, W and D parameters on the basis that $\sim$ 85 % of the γ-ray images fall within these domains, leading to L: 0.18^o - 0.52^o, W: 0.08^o - 0.24^o and D: 0.45^o - 1.25^o.

In Fig. 4a, we show the resulting quality factor Q ($\alpha \leq 15^o$) for the overall data-samples as a function of the image size, S. It is found that Q increases with S, first gradually, reaching a value Q $\sim$ 6 at S $\geq$60 pe, and then more rapidly, eventually attaining a value Q $\sim$ 11.5 at S $\geq$ 140 pe. The apparent dependence of Q on S, as inferred from Fig.4a, can be understood as a consequence of larger number of higher energy primaries contributing to larger S values. On the basis of the plot in Fig.4a, we may define an effective image gamma-ray threshold energy ($E_{\gamma min}$) for the IE as corresponding to Q $\geq$ 8, beyond which Q increases more rapidly, as stated above. As is evident from Fig.4a, for the TACTIC Imaging Element, $E_{\gamma min}$ turns out to be $\sim$ 1.0 TeV on this basis,corresponding to $< S > \sim$ 80 pe (equation 1 above).

Figures.4b and 4c show, as a function of S, the corresponding percentages of γ-ray and proton-images retained in the database samples filtered as per the above-referred

image-selection criteria. It is evident that, in the present case, the fraction of gamma-ray (signal) images retained lies between 50 - 30 % for S = 20 - 140 pe and for $\alpha \leq 15^o$, while the corresponding number of p-images decreases from $\sim$ 1.06 % for S >20 pe, to $\sim$ 0.07 % for S >140 pe. Taking Q $\sim$ 8.5 as a reasonable value for the figure of merit of the Imaging Element, the on-source time required for the extraction of the γ-ray signal, from the standard cosmic γ-ray candle, Crab Nebula, turns out to be $\sim$ 4 hrs at 5 σ confidence level. The maximum value of Q, suggested by the present simulation studies (Fig. 4a), is compatible with the value experimentally derived for the IE when it detected a strong γ-ray signal from the Mkn 501 during an observation campaign carried out in April - May, 1997 with a 81-pixel prototype camera [11].

5 Conclusions

Using the CORISKA simulation code-generated gamma-ray and proton images as expected to be recorded by the TACTIC Imaging Element in the sky-noise suppressed situation, the respective domains have been obtained for the two event types for supercuts image parameters, viz, L,W, D and α. The resulting quality factor of the telescope has been estimated as a function of the image size parameter (S) and the γ-ray image-threshold value obtained for the instrument as $\sim$ 1.0 TeV, corresponding to $< S > \sim 80$ pe. For the corresponding value of Q $\sim$ 8.5, the expected retrieval time from the gamma-ray signal from the Crab Nebula turns out to be $\sim$ 4 hours at $\geq$ 5 σ statistical confidence level.The studies are being continued and final results based on use of more sensitive size-dependent, extended supercuts or dynamic cuts and will be presented elsewhere.

References

[1] A.M. Hillas, Proc. 19th ICRC (La Jolla) 3 (1985) 445

[2] C.L. Bhat, Proc. on "Towards a Major Atmospheric Cerenkov Detector-V", O.C.de Jager (ed.), (1997) p.398

[3] S.K.Charagi et al., Exp. Astronomy 11: 71-79 (2001)

[4] C.L.Bhat, A.K.Tickoo, R.Koul and I.K.Kaul., NIM A 340 (1994) 413

[5] D. Heck et al., Report FZKA 6019 Forschungszentrum, (1998) Karlsruhe.

[6] M.L.Sapru et al., (this precedings)

[7] D.J.Fegan, Space Sci. Rev. (1996) 75, 137

[8] S.Sinha, J.Phys. G:Nucl. Phys.,21, 473 (1995)

[9] G.Mohanty et al., Astroparticle Physics 9 (1998) 15-43

[10] D.J. Fegan, J. Phys G: Nucl. Part. Phys. (1997) 23, 1013

[11] C.L.Bhat, Rapporteur Talk at the 25th ICRC (Durban), M.S.Potgieter, B.C.Raubenheimer, D.J.van der Walt, eds. (World Scientific, Singapore, 1997) p.211